

# **Measuring Electrodynamics of the Ionosphere by Digital Ionosondes and Other Techniques**

**B. Reinisch      G. Sales**

**University of Massachusetts/Lowell  
Center for Atmospheric Research  
1 University Avenue  
Lowell, MA 01854**

**September 2000**

**Scientific Report No. 2**

<b>APPROVED FOR PUBLIC RELEASE; DISTRIBUTION IS UNLIMITED.</b>
--



**AIR FORCE RESEARCH LABORATORY  
Space Vehicles Directorate  
29 Randolph Rd  
AIR FORCE MATERIEL COMMAND  
Hanscom AFB, MA 01731-3010**

---

**20021008 172**

This technical report has been reviewed and is approved for publication.



Balkrishna S. Dandekar  
Contract Manager



Carl J. Christensen, Major, USAF  
Acting Chief  
Space Weather Center of Excellence

Qualified requestors may obtain additional copies from the Defense Technical Information Center (DTIC). All others should apply to the National Technical Information Service.

If your address has changed, if you wish to be removed from the mailing list, or if the addressee is no longer employed by your organization, please notify AFRL/VSIM, 29 Randolph Rd., Hanscom AFB, MA 01731-3010. This will assist us in maintaining a current mailing list.

Do not return copies of this report unless contractual obligations or notices on a specific document require that it be returned.

REPORT DOCUMENTATION PAGE					Form Approved OMB No. 0704-0188	
The public reporting burden for this collection of information is estimated to average 1 hour per response, including the time for reviewing instructions, searching existing data sources, gathering and maintaining the data needed, and completing and reviewing the collection of information. Send comments regarding this burden estimate or any other aspect of this collection of information, including suggestions for reducing the burden, to Department of Defense, Washington Headquarters Services, Directorate for Information Operations and Reports (0704-0188), 1215 Jefferson Davis Highway, Suite 1204, Arlington, VA 22202-4302. Respondents should be aware that notwithstanding any other provision of law, no person shall be subject to any penalty for failing to comply with a collection of information if it does not display a currently valid OMB control number.						
1. REPORT DATE (DD-MM-YYYY) 14-07-2000		2. REPORT TYPE Scientific, #2		3. DATES COVERED (From - To) 24 Sep 97-23 Sep 98		
4. TITLE AND SUBTITLE Measuring Electrodynamics of the Ionosphere by Digital Ionosondes and Other Techniques				5a. CONTRACT NUMBER F19628-96-C-0159		
				5b. GRANT NUMBER		
				5c. PROGRAM ELEMENT NUMBER 62601F		
6. AUTHOR(S) Bodo Reinisch, Gary Sales				5d. PROJECT NUMBER 1010		
				5e. TASK NUMBER IC		
				5f. WORK UNIT NUMBER AA		
7. PERFORMING ORGANIZATION NAME(S) AND ADDRESS(ES) University of Massachusetts Lowell Center for Atmospheric Research 600 Suffolk St Lowell, MA 01854				8. PERFORMING ORGANIZATION REPORT NUMBER		
9. SPONSORING/MONITORING AGENCY NAME(S) AND ADDRESS(ES) Air Force Research Laboratory/VSBXI 29 Randolph Road Hanscom AFB, MA 01731-3010				10. SPONSOR/MONITOR'S ACRONYM(S)		
				11. SPONSOR/MONITOR'S REPORT NUMBER(S) AFRL-VS-TR-2002-1556		
12. DISTRIBUTION/AVAILABILITY STATEMENT Approved for Public Release; distribution unlimited						
13. SUPPLEMENTARY NOTES						
14. ABSTRACT <p>The contributions of chemistry and vertical motion to the F-region airglow production were simulated using a relatively simple computer code. Observed emissions inside depletion regions and variations in background emission were studied to try to explain differences in emission between nights when depletions were present and nights when no depletions were present, and also the apparent depression of the ionosphere by 20-30 km before a moving depression arrives at a site.</p> <p>Calculations showed that the much faster SMART code produced signal and signal-to-noise predictions almost as accurate as the HASEL code.</p> <p>Digisonde data from Millstone Hill for four periods from October 1998 through March 1999 were archived.</p> <p>The ARTIST4 program was completed and installed in several DISS systems in the US and elsewhere.</p>						
15. SUBJECT TERMS Airglow F-region Electron depletions						
16. SECURITY CLASSIFICATION OF:			17. LIMITATION OF ABSTRACT	18. NUMBER OF PAGES	19a. NAME OF RESPONSIBLE PERSON Balkrishna S. Dandekar	
a. REPORT UNCL	b. ABSTRACT UNCL	c. THIS PAGE UNCL			19b. TELEPHONE NUMBER (Include area code) (781) 377-2761	

## TABLE OF CONTENTS

<b>1.</b>	<b>INTRODUCTION</b>	<b>1</b>
<b>2.</b>	<b>RESEARCH</b>	<b>2</b>
2.1	STRUCTURE OF THE EQUATORIAL IONOSPHERE	2
2.1.1	Equatorial Depletion Analysis	2
2.1.2	Equatorial Spread F	8
2.2	PROPAGATION ANALYSIS (PROJECT SEND)	8
2.3	DIGISONDE DATABASE	10
2.3.1	Archiving the Digisonde Database	10
2.3.2	Developments of Internet access of SAO data from Digisonde Stations	11
2.4	DIGISONDE NETWORK SUPPORT	16
2.4.1	ARTIST4 Upgrades	16
2.4.2	DISS Network Support	17
2.5	DIGITAL SOUNDER FOR TOPSIDE OBSERVATIONS	18
<b>3.</b>	<b>SUMMARY</b>	<b>21</b>
<b>4.</b>	<b>PUBLICATIONS</b>	<b>22</b>

## 1. INTRODUCTION

The University of Massachusetts Lowell Center for Atmospheric Research (UMLCAR) continues to work towards a better understanding of the physics of the upper atmosphere that can lead to reliable transionospheric and subionospheric communications, meeting the needs of the United States Air Force. With the arrival of networking and super communication highways, space science has been propelled into real-time forecasting. New capabilities will greatly enhance the ability of the United States Air Force to determine when communication systems may be affected by ionospheric and/or solar-terrestrial phenomena. These capabilities, being pursued at UMLCAR in conjunction with other institutions as part of the "Space Weather Forecasting" initiative, are essential for any program designed to use the space-earth environment for reliable future communication requirements.

The task of specifying the ionosphere has been subdivided into several areas. These include:

- **Structure of Equatorial Depletion Bands:**

The plan is to study the morphology of equatorial depletions and to determine the physical cause for their development and behavior. Particular emphasis will be placed on the use of ionosonde and other high frequency (HF) measuring techniques involving both the experimental and theoretical study of these phenomena. The experimental part consists of measurements made with a variety of instruments during the campaigns planned by Air Force Research Laboratory (AFRL) scientists as well as using the routine observations at established equatorial sites such as at Jicamarca, Peru.

- **Polar Cap Monitoring:**

Ionospheric drift measurements from high latitude Digital Ionospheric Sounding System (DISS) stations have shown some correlation between the sign of  $B_z$  and the plasma drift velocity. Ionospheric drift data from digital ionosondes at Qaanaaq, Greenland; Sondrestromfjord, Greenland; Svalbard, Norway; and Goose Bay, Labrador, are used to refine the process of determining the polarity of  $B_z$  from ground-based ionospheric drift measurements. These results are used to develop the polar cap convection patterns.

- **Ionospheric Modification Diagnostics:**

Under this task, UMLCAR will be responsible for deploying the ionospheric diagnostic equipment, conducting measurements and providing quick-look data for the conduct of ionospheric heating experiments and analysis. UMLCAR also provides geophysical interpretation of the data.

- **Field Campaigns:**

Under this task UMLCAR participates in measurements at remote field locations. UMLCAR provides support to AFRL in making joint measurements with other

sensors using the DPS systems. As part of this task, UMLCAR will construct one four-receiver Digisonde Portable Sounder (DPS-4) system with four receive antennas.

- **Development of Digisonde Database:**

UMLCAR collects and provides quality control on electron density profile data for selected periods and locations. These refined data are used to compare with the Air Force Research Laboratory's Parametrized Ionospheric Model (PIM). Also, UMLCAR is developing a standard format for these analyzed Digisonde drift data and archives these data in the Digisonde database.

- **Digisonde Network Support:**

UMLCAR provides upgrading of DISS, AN/FMQ-12 and network support, particularly for building the ionospheric model database.

- **Low Power Digital Portable Sounder (LPD):**

UMLCAR is developing a prototype of a Low Power Digital Ionosonde (less than 100 watts) needed for routine ionospheric measurements.

- **Topside Automated Sounder, TOPAS:**

Under this task, UMLCAR is designing and building a compact and efficient prototype ionosonde for satellite based observations.

- **Propagation Analysis (Project SEND):**

Using analytic ray tracing techniques, UMLCAR was tasked to develop a program for rapid propagation analysis with expected signal-to-noise as an indicator to the USAF user of the expected performance of his HF system.

## **2. RESEARCH**

### **2.1 Structure of the Equatorial Ionosphere**

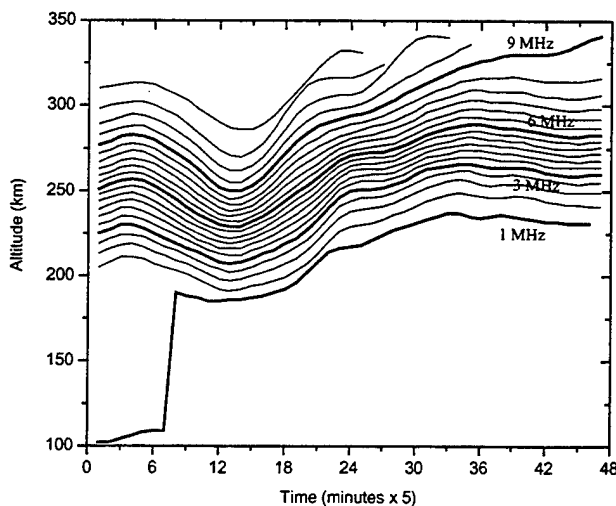
#### **2.1.1 Equatorial Depletion Analysis**

Before attacking the dynamics of the depletion regions observed at Agua Verde, Chile, it was decided to investigate the chemistry and dynamics of the background F-layer as it affects the overall 630.0 nm emission intensity. Following our earlier work involving the chemistry and vertical motions within the F-layer that separated the contribution of each to the observed Doppler shift, it was decided to apply this technique to determine the integrated airglow emission intensity.

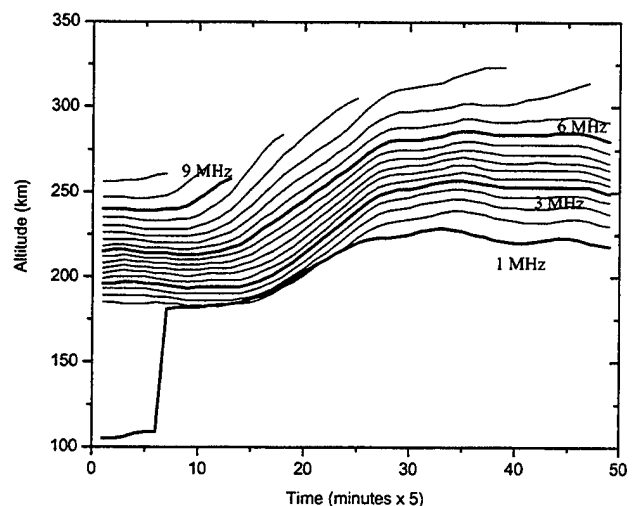
A rather simple model was developed, limited at this stage to post F-region sunset times when it could be assumed that there was no solar production of ionization. Under these conditions in the F-region, the chemistry becomes rather simple and only an electron loss mechanism was considered that involves, first, charge exchange between  $O^+$  and  $O_2$ , that followed by a dissociative recombination reaction which removes the electrons and produces excited atomic oxygen. The  $O^*$  in a forbidden state, after some time, emits a “red” photon and the atomic oxygen returns to the ground state. It is these photons that constitute the observed 630.0 nm airglow.

In addition to the loss of electrons by this recombination process, the redistribution of electrons by vertical transport was considered. Both upward and downward transport were considered. The electron density profiles as a function of time were calculated using the continuity equation including the effects of vertical transport. For this problem, changes in the electron density in the 250 to 300 km altitude regimes were critical as the source region of the airglow. Typically, this altitude range, in the early evening, is at or below the F-layer peak. Assuming that the reaction rates for the chemistry part of this problem are relatively well known (these simulations were run using the reaction rates taken from the rather complete airglow emission program developed by Stan Solomon at the University of Colorado), the measured electron density profiles were fit by varying the vertical transport velocity as a function of time as the input to the continuity (differential) equation. The assumption was made that the transport velocity is constant over the altitude range for this simulation, i.e., 200 to 600 km. The altitude range for integration of the differential equation was made larger than the region of interest, thereby moving the boundary conditions out of the critical region.

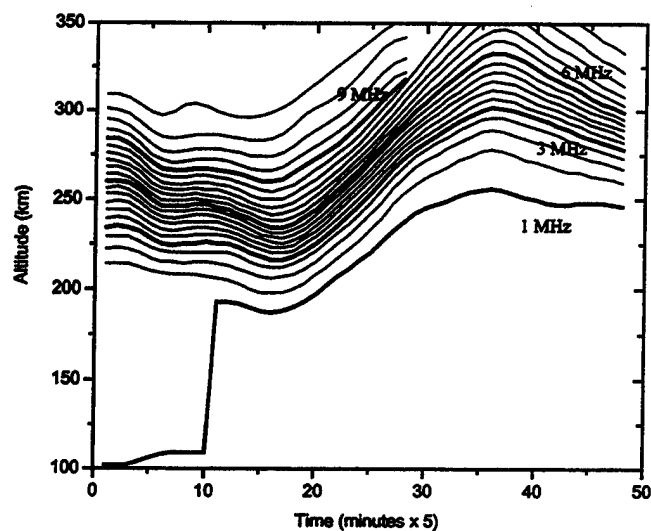
For October 1, 2, and 3, 1994, the measured plasma frequency contours at Agua Verde as a function of time are shown below.



Agua Verde, Chile – Oct 2, 1994



Agua Verde, Chile – Oct 3, 1994



Agua Verde, Chile – Oct 3, 1994

Figure 1. Plasma frequency contours for October 1, 2, and 3, 1994.  
The contours are in 0.5 MHz steps. Time axis begins at 00 UT.

As stated above, the differential equation requires a vertical velocity time profile (assumed uniform with altitude) and after several trials the profile in Figure 2 was used to generate a series of electron density height profiles (the step intervals for the solution of the differential equation were 1 s and 5 km).

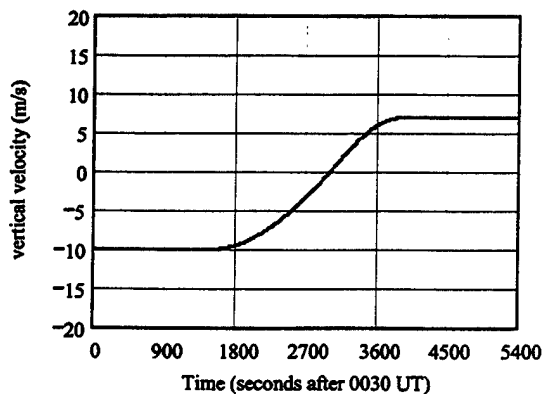


Figure 2. Assumed vertical velocity time profile for October 2, 1994, at Agua Verde.  
The time scale begins at 0030 UT. (Downward is negative)



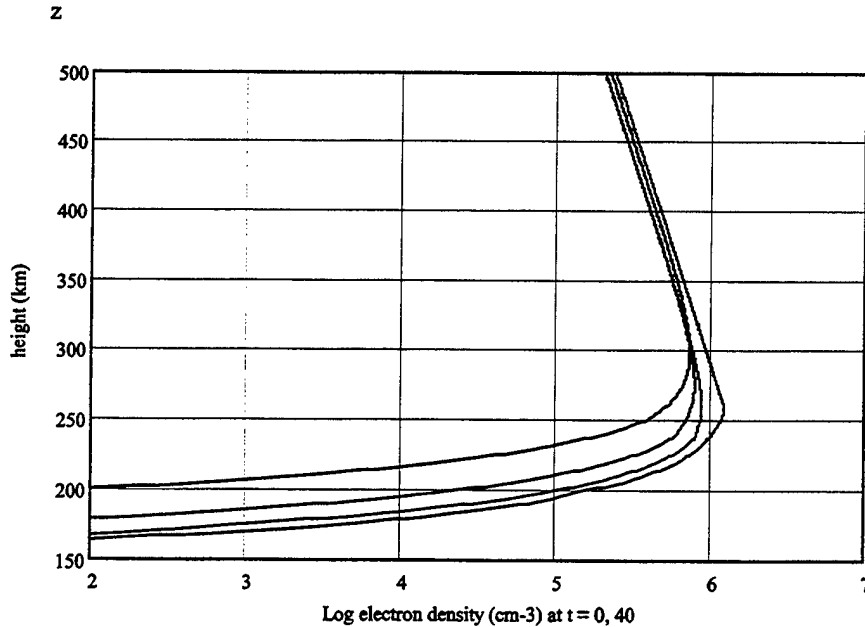


Figure 3. Calculated electron density profiles at 0, 40, 60 and 90 minutes after 0030 UT.

A downward velocity of 10 m/s was assumed to persist for 30 minutes, followed by a 30-minute transition to an upward motion of 7 m/s. The zero vertical velocity was set at  $t = 3000s$ , i.e., at 0120 UT for these particular data. The results of this computation (Figure 3) show a selected sequence of electron density profiles at  $t = 0, 40, 60$  and 90 minutes after the start at 0030 UT.

The volumetric emission rate (photons/cm<sup>3</sup>/s) was calculated using the rate of loss of electrons at each altitude. The results for October 2, 1994, at 0030 UT are shown in Figure 4. In this case, the maximum emission rate of just below 100 (photons/cm<sup>3</sup>/s) occurs at about 240 km with a relatively rapid fall off at lower altitudes and a more gradual decrease above. The calculated emission rate is down by almost a factor of ten at  $\pm 50$  km from the peak altitude. Finally, for each time (one-second steps) the volumetric emission rate is integrated over the altitude range of 200 to 600 km to produce calculated emission intensity for the simulation of the measured optical airglow on the ground. These results are shown in Figure 5.

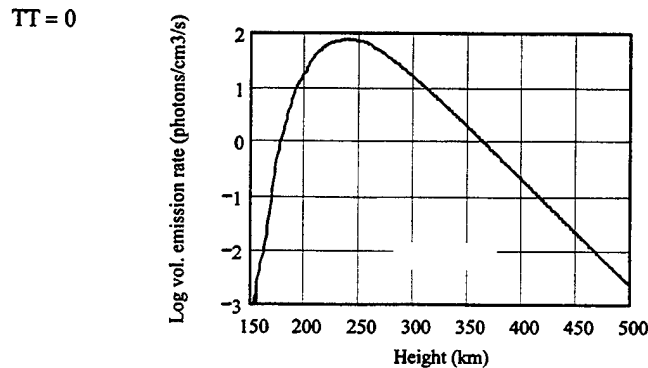


Figure 4. Calculated volumetric emissions rate (630.0 nm) at 0030 UT.

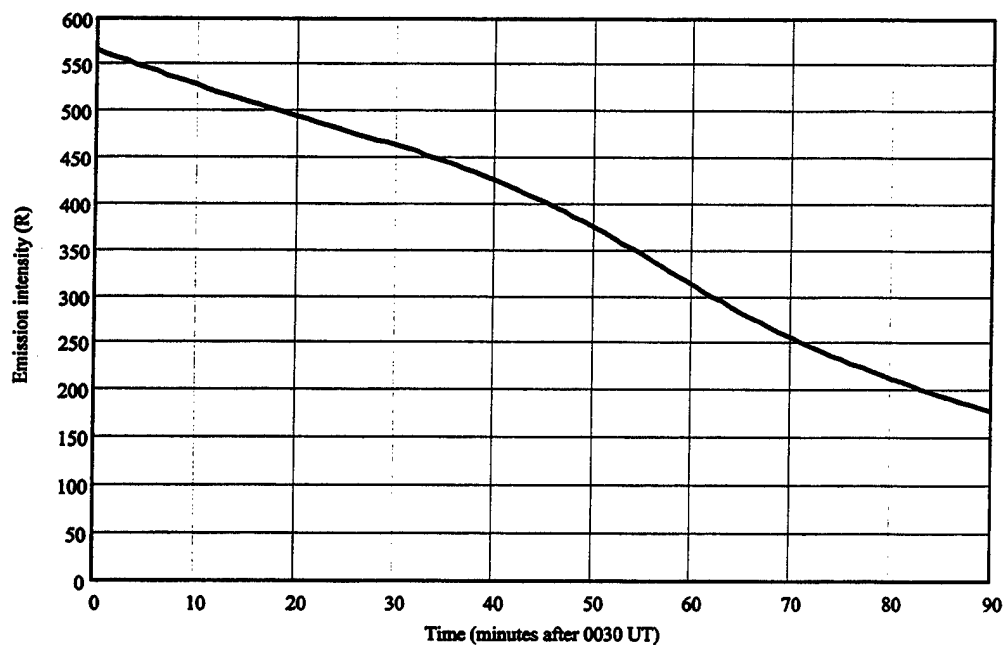


Figure 5. Calculated emission intensity of the 630.0 nm airglow for October 2, 1994, at Agua Verde based on simulated electron density profiles.

Here, the emission intensity begins at 570 R and decreases rather steadily over 90 minutes to about 180 R. Comparing this curve with the measured emission intensity, from 30 minutes to 90 minutes after 00 UT, the general behavior is very similar. The obvious and disturbing part of this comparison was the discrepancy in the absolute value of the emission intensity measured in Rayleighs, differing by more than a factor of 5.

To investigate the problem of the discrepancy between the calculated and the measured emission intensity, it was decided to consider several different approaches.

First, by rerunning the program under different conditions, the theoretical analysis developed at UMLCAR was reexamined. At that point, only the consistency of the several solutions was used to indicate that the program was operating properly. Given these reasonable results and after discussions with E. Weber, it was decided to take the following two directions.

1. Stan Solomon was contacted at the University of Colorado. He has developed an extensive code to calculate the intensity of 630.0 nm emissions in the F-region. His code is considerably more detailed than the one developed here. A meeting was held with Solomon after an AFRL seminar and it was agreed that an electron density profile from Agua Verde would be sent to him for analysis using his emission code. It then would be possible to compare his results with our results.

2. Meetings were held with Peter Ning and his associates from KEO to discuss the calibration of the HAARP scanning photometer. It was agreed that they would look into possible sources for the discrepancy between the CAR simulations and the "measured" emission intensities that were larger, by a factor of 5 or 6.

Working with Solomon to get the details straightened out, the calculated emission intensities, using his elaborate code, were found to be within 10% of our calculated value. Almost simultaneously, the report came back from KEO that they had made a mistake when they believed that they had "averaged" four adjacent pixels to reduce the 512 x 512 array of CCD elements to 256 x 256. Actually, the HAARP system summed the four pixels and did not average them.

Doing the averaging increased the "measured" intensity by a factor of four and we feel that the basic discrepancy has been resolved and have concluded that our simple emission code including vertical drift motions to follow the development of the layer and the associated airglow emission intensity after sunset, performs well. The remaining difference between the measured and calculated intensities, typically 30 to 50 percent, needs to be addressed and may involve adjusting the electron temperature or one of the several other factors in the chemistry of the simulation.

With a simulation code that works reasonably well, it is now possible to investigate the dynamics of the depletion bands, applying the same code with different vertical transport velocity profiles to determine the range of speeds that lead to partially depleted electron density bands. This research addresses the problem of the residual emissions consistently observed inside the depletion bands at Agua Verde.

After resolving the question of the calibration of the photometer and achieving good agreement between the observed emission rates and calculations using the measured electron density profiles and the simplified version of the chemical and transport code, the investigation of the observed emission inside the depletion and the variations of the background emission rate spatially over the sky and from day to day was begun. The data used included both the Digisonde and the all-sky photometer images at 630.0 nm and focused on two problem areas.

1. Understanding the differences between the emission rate on October 2 when no depletions were present (the observed rate was about 2x the background rate measured on October 1 and 3) and on the other nights when several depletions were present during the pre-midnight period.
2. On both nights when depletions were present, there appears to be a depression of the ionosphere of the order of 20 to 30 km before the moving depletion arrives at the site.

The sounder and the all-sky data were reexamined to confirm these observations. These results were presented at the AGU spring meeting in Boston and at the International Union of Radio Science (URSI) meeting in Toronto in August.

### 2.1.2 Equatorial Spread-F

The paper "Pacific Region Equatorial Anomaly Studies in Asia (PREASA)" written by J.L. Scali, K. Igarashi, B.W. Reinisch, H. Minakoshi and Y. Masuda, has been submitted to the Journal of Geophysical Research Space Physics (JGR) for publication. In this paper, ionospheric irregularities associated with a daytime scintillation event observed in the Japan Asian sector during the PREASA-II campaign on 23 February 1997 are described. The scintillation-causing irregularities are identified as small-scale field aligned depletions in the lower  $F$  region. The duration of scintillation is controlled by how rapidly these irregularities are filled in by daytime ionization sources. The triggering mechanism appears to be related to the occurrence of spread sporadic  $E$  and displays propagation speeds from high to low latitudes comparable to medium-scale gravity waves.

## 2.2 Propagation Analysis (Project SEND)

At a recent meeting, the USAF established a new initiative called Project SEND. The requirement was to develop an HF propagation package that was capable of modeling signal, noise and signal-to-noise ratio (SNR) for the coverage area of a communications system at any arbitrary location on the surface of the earth. The approach was to use the Air Force's adjustable ionospheric model, PRISM, in connection with a rapid ray tracing routine. In the particular theater of operation, where the "wanted" transmitter is located, it was assumed that a DISS (vertical sounder) would be available to update PRISM and thereby provide a "real-time" ionosphere for the ray tracing.

The goal was to compute the expected signal level and SNR over a 360 degree azimuthal scan that typically would be provided by the wanted transmitter. These computations were to be available, potentially; to several customers in near real-time (approximately every 15 minutes). It was also necessary to consider the effect of an "unwanted" transmitter operating at the same frequency as the wanted transmitter, effectively trying to jam any receiving system operating at the wanted frequency. This "jammer" was also to have an arbitrary location within the same coverage of the PRISM model as updated by DISS. It was decided that the PRISM area in which the wanted and unwanted transmitters were located would be a 4000 km radius circle around the DISS site.

HASEL, which is the 3-D numerical ray tracing code developed by Chris Coleman at DSTO, Australia, was the first choice. Although this program has great precision, it runs relatively slowly, particularly for this project where it might be required to calculate the coverage for several frequencies for several customers. Each frequency required some 180 azimuthal steps and up to 90 elevation steps or approximately 15,000 rays per frequency per customer. HASEL was too slow and an analytic ray tracing code "SMART" developed at the Defense Research Establishment in the UK was considered.

SMART is an analytic ray tracing code that assumes each altitude slice is quasi-parabolic in shape and it is then possible to have a rapid calculation of the ray path in that segment. Each segment, in altitude and range was modeled in a quasi-parabolic form and the calculated ray paths were extended from the transmitter up to the ionosphere and back to the ground. On a

UNIX-based SGI computer, each frequency (15,000 rays) was calculated in only a few minutes, sufficiently fast to meet the operational requirements.

SMART had two other advantages. First, it calculated the geometrical spreading loss for one and two hops (two hops are required to get the transmitter coverage out to near 4000 km); and second, it calculated the absorption of the radio wave through the lower ionosphere: neither of these features was available with HASEL. SMART also included a grid mapping routine that took the radial array of rays from the transmitter and generated a pixel-by-pixel map for the signal strength or the SNR.

Tests were run to compare the performance of SMART against the more accurate HASEL. For the relatively slowly varying ionospheres generated by PRISM, the SMART results were sufficiently close to HASEL and the listed advantages made the SMART code the smart choice. On the other hand, SMART did not have a noise model and after some research the NOISE.DAT model distributed by the International Telecommunications Union was obtained and incorporated as part of the SEND software package. This computer-based model was the updated version of CCIR 312, which served the radio propagation community for many years. This noise model gives, for any location, season and time of day, the atmospheric noise level at the selected frequency. It also provides the statistics associated with the predicted noise level. This noise code was incorporated into SMART, which then made it possible to compute the SNR at each pixel within the coverage map. NOISE.DAT was also able to estimate the galactic noise component, but galactic noise, typically, lies below atmospheric noise for frequencies below 30 MHz. Finally NOISE.DAT estimates the man-made component of noise depending on the particular environment. This has to be selected from four choices, beginning with the quietest: quiet rural, to rural, to residential and finally to the highest noise level, industrial. Unfortunately, this is a subjective choice, depending on the location of the receive site. Without being able to specify a specific receive site, the default manmade noise level was chosen to be residential and applied everywhere.

Finally, it was decided to modify the absorption model in SMART. The developers of SMART used the typical control point approach, i.e., one point per hop at the mid-path. It was felt that improvements could be made by calculating the absorption on the up leg and the down leg of each hop, separately for each ray. This involved a relatively simple calculation of the location of the point where each ray penetrated the 90 km altitude. Then the geographic coordinates of those points were computed and the contribution to the total absorption was calculated by adding the absorption at each passage point through the D-region. Depending on the time of day and ray path direction, this could amount to several decibels.

The interface between PRISM and SMART has worked very well. With the modifications to the absorption routine and the addition of the ITU noise program, propagation performance maps were generated. The first maps were centered on Hanscom AFB, using the location of that sounder as the center of the map. The output of this program was compared to the full HASEL ray tracing and the results compared very well. Routinely, two maps were available, one for received signal level and the other for signal-to-noise ratio.

These ray tracing calculations were initially carried out in one-degree steps in elevation going from 1° to 90° or until the ray penetrated the ionosphere, and azimuth in one-degree steps, typically from 0° to 360°. The run time was somewhat long and it was decided to increase the azimuthal step size to 2°. This shortened the run time by a factor of two, but because of the spreading of the rays, some areas at the longer ranges were left unfilled.

At this point it was decided to extend these ray tracings out to the full two-hop coverage. To do this the absorption for the two-hop situation had to be modified. With these very long ranges many of the coverage cells (initially 1° latitude by 1° longitude) were left empty, where no ray fell on these cells and resulted in a "Swiss cheese" appearance on the coverage maps. Increasing the PRISM cell size to 2° by 2° mitigated this problem. This also shortened the processing time and now many more of the previously empty cells had rays in them. Another technique was developed to eliminate these stray holes in the propagation pattern. A simple algorithm was used to determine if a particular empty cell had filled neighbors. If the answer was yes, the empty cells were filled, using the average of the surrounding cells. Using these two techniques together produced quite acceptably looking maps. Finally, a three-color scheme was developed to indicate good, average and poor propagation conditions. This was intended as a guide for the unsophisticated user.

## **2.3 DIGISONDE DATABASE**

### **2.3.1 Archiving the Digisonde Database**

The process of archiving of Millstone Hill data continued. Data covering the following time periods was archived on 4 CD-ROMs entitled:

98280 to 98313 (October 07, 1998 to November 09, 1998)  
98314 to 98328 (November 10, 1998 to November 24, 1998)  
98329 to 98360 (November 25, 1998 to December 26, 1998)  
98361 to 99073 (December 27, 1998 to March 14, 1999).

From 2100 UT on 98316 (November 12, 1998) to 1815 UT on 98317 (November 13, 1998) and also from 1600 UT on 98332 (November 28, 1998) to 0200 UT on 98333 (November 29, 1998), the data includes a mixture of Millstone Hill and Hanscom ionograms with overlapping measurement times. This resulted because of a campaign that needed data from both stations. The Station ID in the preface of the Hanscom data was changed from 242 to 042 (the Millstone Hill Station ID) with software written for that purpose, to avoid repeated error messages when the data was edited with ADEP. As usual before archiving Digisonde data on CD-ROM, all the data were run through ADEP to detect corrupted data that ADEP cannot handle. All corrupted data were removed.

The Sondrestrom drift data for the time periods 98201 to 98352 (July 20, 1998 to December 18, 1998) and 98353 to 99104 (December 19, 1998 to April 14, 1999) were also archived on two CD-ROMs. A few minor errors were found in the drift data. The prefaces for the data in file 8234J02A.dft indicated that the data were ionogram data instead of drift data, so

this file was excluded from the one-day files on the CD-ROMs. This error and others were found interspersed with the good data and were corrected or removed.

The Millstone Hill Digisonde data and the Sondrestrom drift data were continuously sent to the UMLCAR data center via FTP and these data were archived on CD-ROMs when sufficient data had accumulated.

Working back in time, Millstone Hill data were archived for the following dates in 6 CD-ROMs:

98118 to 98146 (April 28, 1998 to May 26, 1998)  
98147 to 98157 (May 27, 1998 to June 06, 1998)  
98158 to 98176 (June 07, 1998 to June 25, 1998)  
98177 to 98208 (June 26, 1998 to July 27, 1998)  
98209 to 98260 (July 28, 1998 to September 17, 1998)  
98261 to 98279 (September 18, 1998 to October 06, 1998).

Also, the Millstone Hill Digisonde data and the Sondrestrom drift data continue to be processed and archived. Sondrestrom drift data for the time period 98089 to 98200 (March 30, 1998 to July 19, 1998) were also archived on a CD-ROM.

### **2.3.2 Developments of Internet Access of SAO Data from Digisonde Stations**

The Digisonde online archive data retrieval package consists of an applet providing a secure front end GUI for the client, i.e., Digisonde Online and a CGI program providing on the back end, the search, reading, and HTML page formatting of the requested data. The Digisonde Online (Digisonde OL) was designed to read only Standard Archive Output "SAO" data sets, as specified during the Digisonde Users Training Seminar in cooperation with the World Data Centers. The Internet-enabled Digisonde stations maintain a local database of ionospheric characteristics. The database is structured into one-day files in a Standard Archival Output (SAO) format, and the WWW server of the Digisondes provides software tools for online cataloging and visualization of time series using the SAO data sets in the database. The Digisonde\_OL.class applet was completed.

The implementation of the Text and Settings folders was also completed. A brief description of these folders follows:

Graphics		Text		Settings
Time (UT)	Fof2	Fof1	FoEs	Processing
00:14	8:125	N/A	N/A	Manual
00:14	7.950	N/A	N/A	Manual
00:44	7.613	N/A	N/A	Manual
00:59	7.413	N/A	N/A	Manual
01:14	7.613	N/A	N/A	Manual
01:29	7.414	N/A	N/A	Manual
01:44	7:113	N/A	N/A	Manual
01:59	7:307	N/A	N/A	Manual
02:14	7:406	N/A	N/A	Manual
02:29	7:825	N/A	N/A	Manual
02:44	8:107	N/A	N/A	Manual
02:59	7.903	N/A	N/A	Manual
03:14	7.707	N/A	N/A	Manual
03:29	8.203	N/A	N/A	Manual
03:33	8.306	N/A	N/A	Manual
03:59	8.104	N/A	N/A	Manual
04:14	8.025	N/A	N/A	Manual
04:29	N/A	N/A	N/A	Manual
04:44	N/A	N/A	N/A	Manual
04:59	N/A	N/A	N/A	Manual

Figure 6. Text folder example

The text rendering of the selected data sets (Figure 6) can be observed by clicking on the tab labeled Text of the folder selection. This folder contains the ASCII text values of the parameters selected and plotted on the Graphics folder. The time and parameter identifier is given on the first line. The fields are populated as a new selection is made. The scroll bar allows the client to scroll down to the end of the data set. The column labeled Processing indicates if the selected parameter has been scaled automatically using ARTIST or manually using ADEP. The text display is useful for clients as a means to quickly get at the actual values for further data manipulation. The text can be copied to a client's favorite spread-sheet and/or data file. To do this, the required text is highlighted; copied to an internal buffer, then the buffer dumped to the application or file.



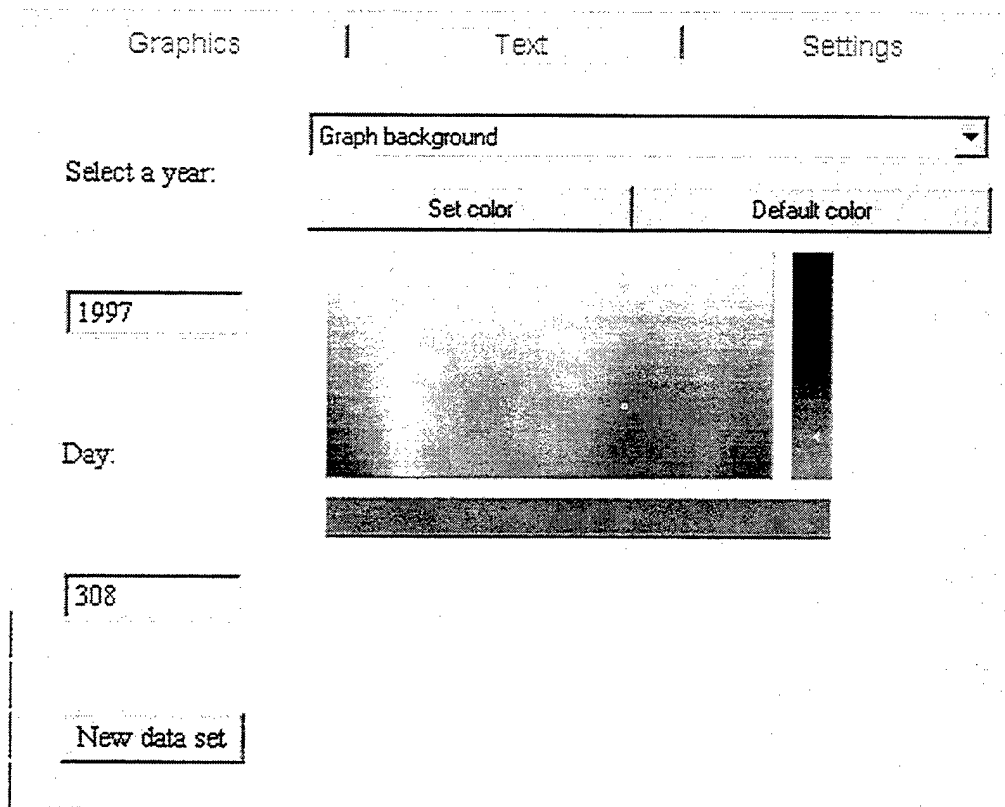
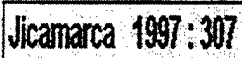



Figure 7. Settings folder example

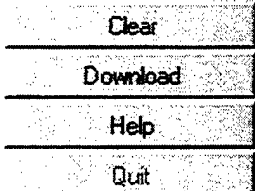
The Settings folder (Figure 7), selected by clicking on the Settings tab, allows the client to change the color-coding of the original graphics display. Clicking the left button on the mouse and running the mouse cursor over the horizontal and/or vertical color bars changes the item's color. The Graphics item is selected using the pull down option above the color bars. The changes are submitted by pressing the "Set color." Pressing the "Default Color" button is used for the original default color settings. This folder also allows the client to choose a new data set. Simply input the required year and day number and press "New data set" button to submit the request. The new data set is loaded automatically and the Text and Graphics folders are reset.

While the applet has internal settings that determine security permissions, the actual delegation or setup of the security model needs to be revisited by the system administrators.

As a detailed overview on how this system works, the Digisonde\_OL applet can be downloaded from the web as part of an HTML document. It begins its life on the web page as a single button labeled "DigisondeDB". Once this button is pressed the applet calls a CGI program (DBscan) to find the most recent data set available to the client. It then unpacks the data and formats a return response within an HTML document. At this point the client would be presented with the main GUI frame. This main frame consists of several components. These are:

	<p>A station name, data set year, and day number header at the top of the applet screen. This allows for rendering multiple views of several data sets from the same station and/or views of data sets from other stations. Every time the “DigisondeDB” button on the original HTML page is pressed a new independent frame would be created.</p>
---	--

	<p>A scrollable parameter selection text field will be supplied to display the parameters available for plotting from the current data set. Double clicking on any parameter loads that specific data set into the text folder and plots it on the graph folder. A limit of five parameters will be allowed on the same graph. An error message would be given if an attempt is made to load any more than five parameters.</p>
---	---

	<p>A set of control buttons will be supplied. These buttons will consist of:</p> <p>Clear: This button allows the client to remove selected parameters individually or all the selected parameters.</p> <p>Download: This button initiates a download using options in the original HTML page from which the applet originated.</p> <p>Help: As the name suggests this opens a help box with information on how to use the Digisonde OL front end.</p> <p>Quit: Closes the frame and releases systems resources.</p>
---	--

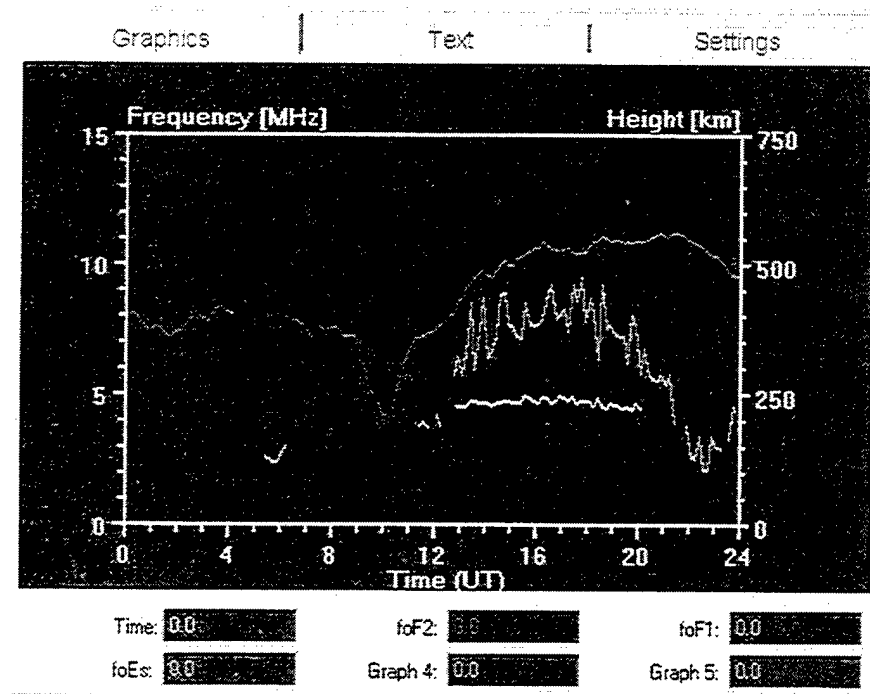


Figure 8. Graph folder example

The Graph folder (Figure 8) is the default folder of three folders that can be selected from the Graphics, Text, and Settings tabs. When a new frame is generated the graphics view of the data set is always loaded by default. This view plots the selected parameter values over a 24-hour period. Universal time is represented along the X-axis, while on the Y-axis, the frequency scale (MHz) is on the left and height scale (km) is on the right.

Below the plot is the text representation of the selected parameters for specific times. When the mouse cursor is moved over the plot, the corresponding time and parameter values for the cursor position will be updated in the text fields. When no parameters are selected the main identifiers in the text area are labeled Time, Graph 1, Graph 2, Graph 3, Graph 4 and Graph 5. As each parameter is selected the labels are updated. As an example, when foF2 is selected as the first parameter, the label Graph 1 will be changed to foF2, and the adjacent text field will be active. Parameter values in these text fields share the same coloring code as the plotted curves for easy identification between graph and text.

These items have been successfully implemented in Java. The Digisonde OL applet used the Java.net and Sun.net class libraries to provide the Application Programming Interface (API) necessary to access Internet and Web resources. Hence these APIs provide a similar approach to distributed computing as a Web Browser in that the applet is able to use the Common Gateway Interface (CGI) to invoke the program "Dbscan.exe" on an HTTP server. The Dbscan.exe currently accepts two arguments, the year and day number. It does a search for the requested data set, unpacks the appropriate SAO file, formats/packs the data into an HTML page and sends the path/filename/and data, back to the client. The DBscan.exe program is written in C++ and is maintained on the Web server generally in the cgi-bin directory.

A local database of ionospheric characteristics was designed to allow for direct access to the time series over the Internet. An archiving scheme was developed to provide and manage the required daily collections of ionogram characteristics. Catalog browsing software was developed to dynamically create availability catalogs for the database contents and allow for data download. A scheme was developed to ensure restricted access to the secure data in the database. Client-side software was developed to provide for interactive visualization of the ionospheric characteristics and data flow control. Data exchange protocols between client and server were modified to provide for a greater number of characteristics for display, proper station identification, and an indicator of data quality validation. A scheme was developed to automatically search for the latest available data in the archive on the first access.

Finally, the introduction of the newer SAO 4.2 format required functional testing of the local Digisonde SAO database support software. The display software had to be modified to allow proper selection and visualization of the new characteristics that were introduced in SAO 4.2.

The characteristic names on the display were brought into agreement with URSI recommendations. Also, these tests showed an inconsistency of operational controls on the display window, which was remedied by introduction of a callback routine monitoring the window "close" event.

## **2.4 DIGISONDE NETWORK SUPPORT**

### **2.4.1 ARTIST4 Upgrades**

For the planned hardware shipment to Chile, techniques for archiving the 16-channel "raw" data from the Digisonde 256 Processor Output computer were investigated. The solution arrived at was to modify the FEND.EXE program in the ARTIST3 software to produce an additional file type, .16c files, when P1 = 6 in the ionogram program. The .16c files would be sent to the ARTIST4 computer where Dispatcher would take care of archiving them.

Specifications for ARTIST4 Phase 2 hardware were developed. The major changes were the substitution of an IOMEGA JAZ drive in place of the Tandberg TDC 3820 tape drive, and the addition of a B&B watchdog timer card. Also an additional 32 megabytes of memory were added to make a total of 64 Megabytes. Additional ARTIST4 computers meeting the above specifications were ordered along with memory, watchdog timer cards, and JAZ drives to update the earlier five computers.

To augment this effort a diagnostic procedures document for the ARTIST4/ARTIST3/network connection was developed. The ARTIST3 portion of Web-based remote control software was developed.

Y2K fixes were made to the processor chassis firmware, some of the ARTIST3 programs, and the ARTIST4 program. Y2K improvements were made to the Timex module, which is used in the DARTIST3.Exe and Dps Control programs. A major activity was to ensure that all of the USAF DISS installations would be Y2K compliant before the end of the 1998. UMLCAR personnel participated in the official USAF Y2K test for the ARTIST4 upgraded

DISS. The test was performed on 28 October 1998 at the Wallops Island, VA DISS site under the supervision of MSgt. Robert Tadena, AFMC SMC Det 11/CID. The tests were successful.

Much Web software was developed for purposes of control of the DISS over the Web and more user-friendly display of data. A Netscape FastTrack server was added to the ARTIST4 package in place of the Microsoft Windows Peer Web Service Web Server. Changes were made to the ARTIST4 cgi scripts to be compatible with the Netscape program.

Also a non-linear frequency scan was developed. Primarily, this required changes to the processor chassis card 2 firmware to select frequencies based on a table. Much thought went into the non-linear frequency table by several individuals based on bandwidth of the Digisonde and critical frequency resolution requirements. The ARTIST3 program that inputs data from the processor chassis, FEND.EXE, was modified to accept the data and pass it on to DARTIST3 and ARTIST4. The Web portion of the Web-based remote control software was developed.

A full security scheme was devised and implemented. The scheme involved configuration of Netscape FastTrack Server, Windows NT, Microsoft Peer Web Services, and Microsoft Remote Access Service (RAS). Different levels of security were provided for Web access, FTP access, and local access depending on the user's permissions.

UMLCAR personnel went to SMALC in Sacramento, CA on 16 November 98 for the purpose of training Dan Rivas and Clay Dukes, SMALC in Sacramento, on the Phase II of the ARTIST4 upgrade to the DISS. Further training and validation of procedures and documentation occurred on 30 November 98 at the Eglin AFB, FL, DISS site. Dan Rivas participated in the upgrade of Phase II of the ARTIST4. Similar training and validation occurred on 2 December 98 at the Ramey Solar Observatory, PR, DISS site. Dan Rivas and Bruce Andrews, from Tobyhanna, PA, Army Depot participated in a complete ARTIST4 installation. On 27 December 98, UMLCAR personnel went to the Bermuda DISS site and did a complete ARTIST4 installation. Discussions were held with the remaining NASA personnel concerning the changes, which would have to be made to accommodate the reduced NASA presence on the island. Instructions were prepared and support was provided to the local personnel at Goose Bay, Canada, and Narssarssuaq, Greenland, so that the local personnel could perform ARTIST4 Phase II upgrades to their DISS installations that had previously been upgraded by UMLCAR personnel to ARTIST4 in August 98. Similarly, instructions and support were provided for local personnel at Sondrestrom and Qaanaaq, Greenland, so that the local personnel could perform complete ARTIST4 installations. Complete ARTIST4 kits were also prepared and shipped to Korea, Australia, England, Italy, Alaska, Sondrestrom, Qaanaaq, Puerto Rico, and Bermuda.

#### **2.4.2 DISS Network Support**

A system for remote control, status visualization and diagnostics of DISS over the standard HTTP layer was designed. A study of dynamic control mechanisms regarding their communications overhead, browser compatibility, hard disk activity and response time was conducted. The control schemes "server push" and "client pull" were evaluated. Both schemes were used to develop alternative software solutions and they were tested side-by-side. The server push technology proved to be more efficient in reporting slow, uneven, or asynchronous data updating. However, unbridgeable compatibility problems were met because the browser

software companies attempt to undermine each other's development by enforcing incompatible interfaces. For this reason the client-pull solution was selected for the final development. To exclude the server from extensive transaction logging activity in the client-pull scenario, the Microsoft server software was changed to Netscape's FastTrack server with a wider range of features. The developed software provides self-updated displays of system status and near real-time ARTIST3 screen capture, as well as the means for remote commanding of the DISS.

A local long-term archive of daily ionospheric data was designed. A data quality control scheme was implemented to ensure valid data formats. Housekeeping procedures were adjusted to include new types of data as well as to maintain an archive of data with format errors. A new archival media was introduced for easier access to the long-term archive. System control software was modified to collect and display the media status.

The new preface data format was designed to accommodate the year 2000 transition. Data handling routines were modified to include new types of automatically scaled information and to operate with a new Y2K-compliant format of system settings. Additions to the DISS control panel were made to include online ARMENU editor and extended screen capture history displays.

Provisions were made in the Sondrestrom ARTIST4 configuration so that local personnel could have access to and be able to control the DISS. Also, provisions were made so that several scientific organizations could access real-time data.

## **2.5 Digital Sounder for Topside Observations**

### **Special Topic – Staggered Pulse Sequences, Basic Relationships**

#### **Introduction**

The Staggered Pulse Sequence (SPS) waveform is investigated for possible deployment in topside sounders. It consists of pseudo-randomly spaced single pulses, each with a pulse width:

$$W = 1 / (\text{receiver bandwidth}).$$

The pulse width should be sufficiently narrow to resolve multiple echo sources separated by a resolution distance:

$$\Delta R = W * c/2,$$

where  $c$  is the speed of light. The pseudo-random spacing is such that echoes from previously transmitted pulses are received between the transmission of subsequent pulses. Since echoes may come from any range, some of the pulse echoes are obscured (in a monostatic configuration) by the subsequent transmitter pulses, so the pulse pattern has to be such that an equal number of echoes are available from all ranges. Another complication of this scheme is that at times corresponding to an echo from one source from pulse "i", another echo from a second source,

from a different range and in response to pulse, "j", may be arriving simultaneously. Therefore the optimum pattern for these pulses would provide a nearly equal number of clear echoes from every range and will create a minimum number (or assuming all ranges are of equal importance, an evenly distributed number) of spurious echoes when sources exist at more than one range.

The signal processing gain is realized by coherently integrating the received echoes. Since the moving sources results in a constantly changing phase in the echo signals, this integration must be performed in the frequency domain. Since the pulse echoes arrive at variable (pseudo-random) intervals, the spectrum-integration task becomes one of estimating the spectrum at each range from a set of non-uniformly spaced samples.

There are many parameters, each of which can be specified over a wide range, and the problem of optimizing the design must be thought out before attempting to define particular parameters. The design must include:

1. The determination of number of pulses in the sequence.
2. The duty factor for those pulses.
3. The desired minimum number of clear echoes from each range to be integrated, thereby realizing a particular signal processing gain.
4. The length of the sequence, which gives the time over which echo pulses can be integrated.

### **Spectral Characteristics**

Of course, another significant part of the design was to specify the spectrum-integration technique, which will be addressed later. Suffice it to say that one of the requirements coming from the spectrum-integration task is that there be a minimum gap between available samples at every range and that the spacing of the available samples is as random as possible, i.e., all auto correlation lags are equally well represented. Further considerations are that the pulses need to span a sufficient time interval (the coherent integration time or CIT) to provide the desired Doppler resolution when the N pulses are coherently integrated.

### **Basic Relationships**

The number of clear echoes (C) is proportional to the number of echoes transmitted (N) and the duty factor of the transmissions (D). If the total time of the pulse sequence is M, in units of time slots, each of width W, from the range resolution considerations described above, the duty factor can be expressed as:

$$D = N/M.$$

Since the reception of  $X = DN$  echo pulses will be blocked due to subsequent transmissions, the expected number of clear pulse echoes at each range is approximately:

$$C = (N-DN) = N(1-D).$$

Next, the number of spurious echoes from other ranges that contaminate samples made at times corresponding to the delayed pulse pattern received from range  $R$  was considered. In general, if there are many echo sources at different ranges, echoes from other ranges only occur infrequently (based on the duty factor,  $D$ ) at sample times corresponding to the range being processed. First, consider the case of two distinct echo sources, the wanted echo at range  $R$  (assuming we are currently echo detecting for range  $R$ ) and a spurious source at range  $S$ . If there was more than one echo from range  $S$  they integrate coherently (although, in general at a different spectral line) when a full spectral integration is made. The probability of an echo from range,  $S$ , falling at a time interval corresponding to another echo from range  $R$  is equal to the duty factor,  $D$ . That is, the lower the density of pulses traveling to and from the echo sources, the lower the joint probability of two echoes arriving simultaneously. However, since we are discussing the particular time at which an echo from  $R$  is being received, it is not the joint probability, but the conditional probability that determines how likely it is that an echo from  $S$  is also present. As was shown above, there were  $N(1-D)$  clear echoes from  $R$ , and in them will be  $N(1-D)D$  spurious echoes from range  $S$ . Therefore, the ratio of wanted echoes to spurious echoes from any other range is simply  $D$ . Therefore, it can be conclude that:

1. If a processing gain  $G$  is desired,  $C$  pulses must be received to achieve this.
2. To reduce spurious interference the time  $M$  over which the  $C$  pulses are received should be stretched out as much as possible to lower the duty factor.

Assuming that the Doppler analysis range is very large compared to actual signal Doppler, it would be advantageous to apply an interpulse phase code at transmission, so that the leakage observed at one range due to pulses from another changes phase rapidly. The phase of the wanted echoes must be inverted upon reception to compensate for the phase reversals modulated onto the transmitted signal; then the cross-talk echoes will arrive with random phase. A near optimum pseudo-random code has been generated for the 768 time-slot code that improves the cross-talk leakage by randomizing the spectrum. This improves the narrowband spectral signal (from the wanted range) to leakage ratio.

The practical limits on low duty factor are the desired speed of the measurement and the temporal coherence of the medium propagating the signal. As noted above, in the section on "Spectral Characteristics," the Doppler resolution and Doppler range (respectively, the inverse of the CIT and the inverse of the closest pulse spacing) are affected by the length of the sequence ( $M$ ). If a very high Doppler range is required it may be necessary to allow pulses to occupy adjacent time slots in groups of 1, 2, 3 or possibly a greater number of transmitter pulses. However, here only the specific case of single pulse, spaced by at least two receiver (quiet) time slots was considered. Two time slots are needed since there is generally a receiver recovery time of at least one time slot before echoes can be received.



Next, the possibility of many spurious echoes arriving from different ranges,  $S_1, S_2, \dots, S_p$  was considered. In general the phase and its first derivative, the Doppler shift, of spurious echoes arriving from various ranges are independent and therefore sum up incoherently in the spectrum-integration process, so that the effect of multiple sources is only large if too many ranges provide echoes. Now it is necessary to compare the range leakage characteristics of SPS to conventional pulse/Doppler radars transmitting a pulse train (e.g., 64 or 128 pulses) and coherently integrating the received echoes. In most radar geometries there is a maximum range ( $R_{MAX}$ ) that provides echoes, or beyond which the echoes are too weak to be detected. Usually the pulse repetition rate is chosen such that all possible pulse echoes are received before another pulse in the pulse train is transmitted, thus avoiding range ambiguity and range aliasing. A ratio of  $M$  to  $R_{MAX}$  was quantified that describes how the pulse density (the duty factor) can be varied all the way to the case of the conventional radar as a limiting case of the SPS parameters. The conventional radar sends one pulse per  $T_{MAX}$ , the time delay associated with the echo from  $R_{MAX}$ , where  $T_{MAX} = R_{MAX} / (c/2)$ .

In the case of SPS, the transmitted code sequence is much longer than the number of ranges of interest ( $M(c/2) > R_{MAX}$ ). Therefore as echoes are received near the end of the SPS sequence, it is not likely to receive any very long delayed echoes from the pulses transmitted near the beginning of the sequence. In the analysis shown below, the search for spurious echoes to ranges less than 256 have been cut off. This tradeoff has already been taken into account in the expressions for spurious echo density above in that the lower duty factor results in a longer sequence and the longer sequence has a lower density of spurious echoes at each range. Therefore of the number of previously transmitted pulses ( $iD$ , where "i" is index of the time slot at which a clear echo is received), only a certain number of them (on the average over the entire sequence,  $R_{MAX} / M \cdot N$ ) may end up as spurious echoes. However, if the ratio of  $M$  to  $R_{MAX}$  is high a large number of spurious echoes will never be seen. Of course one of the limiting cases of a very low duty factor (which results in a very large ratio of  $M/R_{MAX}$ ) is the conventional low PRF design where spurious echoes are never seen because they come from ranges that do not exist or cannot be detected.

### 3. SUMMARY

Progress has been made on modeling the equatorial airglow using a relatively simple set of differential equations. This approach has made it possible to generate electron density profiles and emission profiles as a function of time, particularly after sunset. These calculations generate the background electron density and 630.0 nm emission as a function of time in which the depletions are embedded. The equations controlling the electron density variation with height and time require a vertical velocity profile input. This means that by comparing the calculated electron density profiles with the measured ones, it is possible to generate a reasonable velocity profile. These results ultimately can be used to determine the associated electric field in the F-region that drives the layer up or down.

A new project was added to this year's effort involving propagation analysis over a wide coverage area. Project SEND was designed to evaluate, using the best updated ionospheric models and rapid ray tracing software, the effectiveness of a particular communications system in providing service within the coverage area. The program allows users to effectively manage frequency and power of their systems in an almost real-time environment. Considerable effort

was required to evaluate different ray tracing schemes and ionospheric modeling techniques. Additions to the software models were made to achieve the desired goals. It only remains to test the operational software and evaluate its performance in the real world. On the basis of these tests, some refinements to the code are expected.

Considerable effort was expended this year in getting the Air Force's DISS network "on line," addressing questions on data format, security and ease of access. The Y2k issue was addressed and software modifications made and tested to demonstrate that the Digisonde network would operate successfully through the year 2000 transition. The ARTIST4 program was completed and installed in several of the DISS systems in the US and elsewhere. The SAO formatting and the ARTIST4 package make the Digisonde network very effective in providing a global sounding system that serves both the US Air Force and the scientific researchers who require these data.

Finally, as part of the design of the new topside sounding system a new waveform was introduced involving staggered pulse sequencing. The effectiveness of this proposed waveform was demonstrated in terms of its range and Doppler performance.

#### **4. PUBLICATIONS**

A number of papers reporting our research were published during the report period:

Radicella, S.M., D. Bilitza, B.W. Reinisch, J.O. Adeniyi, M.E. Mosert Gonzalez, B. Zolesi, M.L. Zhang, and S.R. Zhang, IRI Task Force Activity at ICTP: Proposed improvements for the IRI region below the F peak, *Adv. Space Res.*, **22**, 6, 731-739, 1998.

Reinisch, B.W. and X. Huang, Finding better  $B_0$  and  $B_1$  parameters for the IRI F2-profile function, *Adv. Space Res.*, **22**, 6, 741-747, 1998.

Reinisch, B.W., J.L. Scali, and D.M. Haines, Ionospheric drift measurements with ionosondes, *Annali di Geofisica*, **41**, N. 5-6, 695-702, 1998.

Valladares, C.E., R. Sheehan, D.T. Decker, D.N. Anderson, T. Bullett, and B.W. Reinisch, Formation of polar cap patches with north-to-south transitions of the interplanetary magnetic field, *J. Geophys. Res.*, **103**, A7, 14,657-14,670 1998.

Anderson, D.N., M.J. Buonsanto, M. Codrescu, D. Decker, C.G. Fesen, T.J. Fuller-Rowell, B.W. Reinisch, P.G. Richards, R.G. Roble, R.W. Schunk, and J.J. Sojka, Intercomparison of physical models and observations of the ionosphere, *J. Geophys. Res.*, **103**, A2, 2179-2192, 1998.

Reinisch, B.W., 'CHARS': URSI IIWG format for archiving monthly ionospheric characteristics, INAG Bulletin No. 62, WDC-A for STP, Boulder, CO, 38-46, 1998a.

Reinisch, B.W., SAO (Standard ADEP Output) format for ionogram scaled data archiving, INAG Bulletin No. 62, WEC-A for STP, Boulder, CO, 47-58, 1998b.